Influence of lubricant on screw preload and stresses in a finite element model for a dental implant

Jörn, Daniela ; Kohorst, Philipp ; Besdo, Silke ; Rücker, Martin ; Stiesch, Meike ; Borchers, Lothar

Abstract: STATEMENT OF PROBLEM: Loosening or fracture of the abutment screw are frequent complications in implant dentistry and are detrimental to the long-term success of the restorations. However, little is known about the factors influencing the stability of the screw-abutment complex. PURPOSE: The purpose of this study was to investigate the influence of lubricant action during implant assembly on screw preload and stresses in a dental implant-abutment complex. MATERIAL AND METHODS: A dental implant was modeled for finite element stress analysis. Different friction coefficients (=0.2 to 0.5) were chosen for the interfaces between implant components to simulate lubricant action or dry conditions. The stress analyses were each divided into 2 load steps. First, the abutment screw was virtually tightened with a torque of 25 Ncm. This was achieved by applying an equivalent preload calculated according to the different friction coefficients chosen. Second, the construction was externally loaded with a force of 200 N inclined by 30 degrees relative to the implant axis. RESULTS: The screw preload increased with the decreasing friction coefficient. In all components, stresses increased with decreasing friction coefficient. Plastic deformation was observed at the implant neck in an area that expanded with decreasing friction coefficient. No plastic deformation occurred in the abutment. CONCLUSIONS: The results of this study indicated that screw preload should be included in the finite element analysis of dental implants for a realistic evaluation of stresses in the implant-abutment complex. The friction coefficient significantly influenced the screw preload value and modified the stresses in the implant-abutment complex.

DOI: https://doi.org/10.1016/j.prosdent.2013.10.016

Originally published at:
Jörn, Daniela; Kohorst, Philipp; Besdo, Silke; Rücker, Martin; Stiesch, Meike; Borchers, Lothar (2014). Influence of lubricant on screw preload and stresses in a finite element model for a dental implant. Journal of Prosthetic Dentistry, 112(2):340-348.
DOI: https://doi.org/10.1016/j.prosdent.2013.10.016

JPD-13-169

Influence of lubricant on screw preload and stresses in a finite element model for a dental implant

Daniela Jörn, MSc,a Philipp Kohorst, DMD,b Silke Besdo, DEng, MSc,c Martin Rücker, MD, DMD,d Meike Stiesch, DMD,e and Lothar Borchers, DEng, MSc,f
Hannover Medical School, Hannover, Germany; Leibniz University Hannover, Hannover, Germany

aScientific Assistant, Department of Prosthetic Dentistry and Biomedical Materials Science, Hannover Medical School.
bAssociate Professor, Department of Prosthetic Dentistry and Biomedical Materials Science, Hannover Medical School.
cAssistant Professor, Institute of Continuum Mechanics, Leibniz University Hannover.
dAssociate Professor, Department of Cranio-Maxillofacial Surgery, Hannover Medical School.
eProfessor, Head of Department of Prosthetic Dentistry and Biomedical Materials Science, Hannover Medical School.
fSenior Lecturer, Department of Prosthetic Dentistry and Biomedical Materials Science, Hannover Medical School.

This study was additionally supported within the framework of ‘‘Sonderforschungsbereich 599’’ by a grant from the German Research Foundation.

ABSTRACT

Statement of problem. Loosening or fracture of the abutment screw are frequent complications in implant dentistry and are detrimental to the long-term success of the restorations. However, little is known about the factors influencing the stability of the screw-abutment complex.

Purpose. The purpose of this study was to investigate the influence of lubricant action during implant assembly on screw preload and stresses in a dental implant-abutment complex.

Material and methods. A dental implant was modeled for finite element stress analysis. Different friction coefficients (μ=0.2 to 0.5) were chosen for the interfaces between implant components to simulate lubricant action or dry conditions. The stress analyses were each divided into 2 load steps. Firstly, the abutment screw was virtually tightened with a torque of 25 Ncm. This was achieved by applying an equivalent preload calculated according to the different friction coefficients chosen. Secondly, the construction was externally loaded with a force of 200 N inclined by 30 degrees relative to the implant axis.

Results. The screw preload increased with the decreasing friction coefficient. In all components, stresses increased with the decreasing friction coefficient. Plastic deformation was observed at the implant neck in an area which expanded with the decreasing friction coefficient. No plastic deformation occurred in the abutment.

Conclusions. The results of this study indicated that the screw preload should to be included in FEA of dental implants for a realistic evaluation of stresses in the implant-abutment complex. The friction coefficient significantly influenced the screw preload value and modified the stresses in the implant-abutment complex.

CLINICAL IMPLICATIONS

During the clinical assembly of the implant and abutment, lubricants such as saliva may easily contaminate the interface between these components. The use of specific lubricants, appropriate to specified torque settings, may be advantageous, however, dry conditions are generally indicated during abutment insertion.

INTRODUCTION

The joint design of a dental implant complex is aimed at forming a tight connection between all assembly parts and at establishing sufficient resistance against external forces.1,2 The resistance is influenced by the tightening torque applied at the head of the screw, inducing compression at the interfaces between the screw head and abutment and between the corresponding threads of the abutment screw and implant.3 The resulting tensile force built up inside the abutment screw, the so-called preload, is equivalent to a prestress in the screw which should be in the range of 60% to 75% of the material's yield strength in order to resist dynamic loading and to prevent screw loosening.1,4 The preload exerted on the screw not only depends on the tightening torque but also on friction at the interfaces of contacting surfaces5 in the assembly. A low friction coefficient at the contacting faces leads to a higher preload in the abutment screw than a high friction coefficient, when the same tightening torque is applyied.4,6,7 Apart from theoretical considerations, this was demonstrated in an in vitro study by Guzaitis et al,8 in which the friction coefficient was reduced by surface morphology changes due to repeated screw joint closing and opening. Numerous parameters influence friction at the interfaces,9,10 including the hardness of the implant materials, the surface treatments, the type of material, the saliva (lubricants), the speed at which the screw is tightened, the fit between the screw threads involved, the fit at the seat of the abutment and screw, and the tolerances of the

screw shaft and bore hole. These different influences on friction make it difficult to know the exact friction coefficient for a specific situation. Thus, a friction coefficient between 0.2 and 0.5 have been reported for titanium and titanium alloy interfaces, depending on tribological conditions.11-15 This may explain the wide range of friction coefficients - from 0.16 to 0.5 - used for titanium and titanium alloys in finite element analysis (FEA) studies.7,16-21 Many FEA studies have been done,7,16-25 but only a few7,16,17,24,25 have focused on screw preloading in the implant-abutment complex. Lang et al7 and Guda et al24 performed FEA with different implant systems, determining the preloads obtained by simulating the application of the prescribed tightening torque. Variations in friction coefficients have proved to have a large influence on screw preload. However, in these studies, stresses in implant components were not calculated and functional load was not considered. In further FEA studies, Alkan et al16 Merz et al25 and Wang et al17 each applied a single preload calculated with a given friction coefficient. Alkan et al16and Merz et al25 considered additional functional load and calculated stresses either in the abutment and prosthetic screw16 or in the implant-abutment connection,25 whereas Wang et al17 evaluated stresses in a Brånemark III system after screw tightening only. None of these studies, however, evaluated the combined influence of preload and functional load on stresses on implants and abutments under varying frictional conditions during screw tightening.

In the present investigation, the assembly and static loading of an implant-abutment complex were simulated with 3-dimensional, non-linear FEA, allowing for friction between implant parts and possible plastic deformation, by applying a bilinear constitutive law26,27 for the metallic model parts.

Materials and Methods

Geometry

An implant-abutment complex (OsseoSpeed implant 4.5, 13 mm, TiDesign abutment 4.5/5.0; ø 5.5, 1.5 mm, Dentsply Implants) was modeled in a loading situation according to ISO 1480128 (Fig. 1). Geometrical data for the implant, abutment, and abutment screw were supplied in International Graphics Exchange Specification (IGES) format by the manufacturer and processed in the computer-aided design (CAD) part of the finite element program later used for stress analysis (ANSYS Workbench 14.0, ANSYS Inc). To save computation time, the complexity of the model was reduced by omitting the microthread at the neck of the implant body and by modeling the abutment screw shaft as a cylinder with the outer diameter of the thread; this was equivalent to filling the thread with material to a depth of approximately 0.2 mm. The lower portion of the shaft was considered as being bonded to the inner thread of the fixture (see Fig. 1). This may have influenced the stresses in the screw itself but is thought to have negligible influence on the stresses in the implant and abutment because the realistic preload determined by equation 3 was nevertheless applied. The layer of fixing cement between the loading cap and abutment was ignored.

Assignment of material properties

Linear elastic material behavior was assumed for the load cap29 and embedding resin;23 however, for the abutment,26 implant,26 and abutment screw,27 plastic deformation was taken into account by using bilinear stress-strain curves. Table I lists the materials with their specifications. The material data for the abutment, implant and abutment screw were provided by the manufacturer, except for the values referenced in the table. The tangent modulus (Em)

needed for the complete characterization of the metal behavior was calculated by using the following equation:

$$E_m = \frac{(R_m - R_{p0.2})}{(\varepsilon_m - \varepsilon_{p0.2})}, \quad (1)$$

with Rm being the ultimate strength, Rp0.2 the yield strength, and εm the ultimate strain. The yield strain εp0.2 results from

$$\varepsilon_{p0.2} = R_{p0} \cdot \frac{2}{E}, \quad (2)$$

where E is Young modulus.

Simulation parameters, contact and boundary conditions

Semi-automatic meshing was performed by using tetrahedral solid elements with quadratic trial function (element type SOLID187). The mesh consisted of a total of 347 515 elements and 531 639 nodes. Table II lists the number of elements for the model parts. Figure 2 shows the meshed model in a cross-sectional view. Sliding contact with friction was introduced between the abutment and implant and between the screw head and screw seat in the implant. All other contacting faces of neighboring parts were considered bonded. The bottom nodes of the embedding resin were held fixed to ensure the static equilibrium of the model.

Set-up of the analyses

Load application in the analyses was generally divided into 2 main steps. In the first load step, the appropriate tightening torque was simulated by a corresponding preload applied on the shaft of the screw. For this purpose, the screw preload FP was calculated with the following formula according to Bickford et al:9

$$F_P = \frac{T_A}{0{,}159 \cdot P + \frac{d_S \cdot \mu_T}{2 \cdot \cos\left(\frac{\alpha}{2}\right)} + \frac{d_H + d_B}{4} \cdot \mu_H}, \qquad (3)$$

where TA is the tightening torque, P the thread pitch, dS the screw shaft diameter, μT the friction coefficient at the thread, α the flank angle, dH the head diameter, dB the bore diameter, and μH the friction coefficient at the screw head. For the calculation, characteristic screw data were taken from the CAD file, that is 0.4 mm (P), 1.83 mm (dS), 60 degrees (α), 2.35 mm (dH,) and 2.03 mm (dB). Friction coefficients μT and μH were each considered equal to the friction coefficient assumed for the other contact pairs in the model. In order to simulate different frictional conditions during the assembly of the implant and abutment, the friction coefficient for titanium and Ti-6Al-4V was varied between 0.2 (presence of saliva as a lubricant) and 0.5 (dry condition) in steps of 0.1, and the screw preload was calculated accordingly (see Table III). This set of coefficients was chosen to represent the different range of values given in the literature (between 0.1 and 0.4 for lubricated interfaces11,12,30 and between 0.3 and 0.5 for dry conditions13,14,31). In the second load step, an additional external 30-degree off-axis force (see Fig. 1) was applied to the loading cap and incrementally increased up to 200 N. The force was directed towards the beveled face of the abutment, simulating a posterior implant position in the mandible.

Evaluation of results

In order to gain insight into the behavior of the screw during tightening and loading, the force borne by the shaft was evaluated during the first and second load steps. To compare the analyses of the model with varying friction coefficients, the von Mises stresses were evaluated in selected areas of the abutment and implant. In the abutment, regions with high stresses after screw tightening (at the interface with the screw) and after external loading (at the abutment

hexagon) were chosen for further investigation. In the implant, stresses at a path along its upper internal edge were evaluated after each load step. This region is essential for a tight connection between the abutment and implant and has been shown to exhibit plastic deformation under high loads in other studies.23,32,33

RESULTS

Having reached the preload according to Table III during tightening, the load borne by the screw shaft decreased with an increase in the external load (Fig. 3). In all situations, the decrease amounted to more than 37% of the original preload. Figure 4 shows the distributions of the von Mises stresses in the abutment after the first and second load steps as a function of the friction coefficient. For each load step, all distributions shown are qualitatively similar but different in stress levels, and peak stresses increased with a decreasing friction coefficient. After screw tightening, the highest stresses were found at the seat of the abutment screw, with values of approximately 444 MPa (μ=0.2), 311 MPa (μ=0.3), 240 MPa (μ=0.4), and 194 MPa (μ=0.5). In contrast, stress peaks after external loading were located at the edge of the hexagonal index on the side of the force application (Fig. 4, lower part). The stresses along one edge of the hexagon on this side are shown in more detail in Figure 5. With the friction coefficient decreasing from 0.5 to 0.3, the average von Mises stresses along this path first decreased from 342 MPa to 279 MPa, then rose again almost to the starting level when μ was set to 0.2. In any situation and for all conditions, only minor stresses arose in the coronal part of the abutment. The von Mises stresses within the implant after the first and second load step are shown in Figure 6. After screw tightening, the highest stresses appeared at the upper edge of the transition zone from the abutment screw to the implant body. These stresses were almost evenly distributed around the

circumference of the screw bore and decreased with an increasing friction coefficient, from an average of 413 MPa (μ=0.2) to 179 MPa (μ=0.5). Stresses at the upper edge of the implant neck qualitatively showed the same behavior, but at a lower level, ranging from around 282 MPa (μ=0.2) to 71 MPa (μ=0.5) (Fig. 7). Stresses in the lower implant body proved to be negligible in all 4 analyses. After the second load step (Fig. 6 lower half), maximum von Mises stresses were found at the upper edge of the implant neck. Due to the oblique loading, the abutment was pressed against the buccal inner wall of the implant, resulting in compressive stresses in this area. The von Mises stresses partially reached the yield strength of the material (483 MPa), presumably leading to plastic deformation (see also Fig. 8). The region of possible plastic deformation increased with a decreasing friction coefficient, as can be seen in the lower half of Figure 6 and also in the corresponding stress profiles shown in Figure 8, where the yield strength was reached at 16% of the path length for μ=0.5 and at 30% of the path length for μ=0.2.

DISCUSSION

Reducing the friction coefficient, which could, for example, occur by saliva infiltration, increased stresses in the implant-abutment complex and can lead to plastic deformation at the implant neck during loading.

In this FEA study, certain simplifications and assumptions were made which might have influenced the calculated stresses. The first approximation consisted of cutting off the 0.1 mm deep microthread at the neck of the implant body, resulting in slightly more resilient abutment support by the surrounding implant neck. In consequence, local stresses might have been slightly overestimated in the analyses presented. Secondly, contrary to the studies of Lang et al7 and Wang et al,17 the abutment screw threads were omitted. This is most likely to influence only

stresses in the direct surroundings of the thread and to leave the rest of the stress distribution intact. Moreover, the screw preload calculated here for a friction coefficient of 0.2 (506 N) is of the order of that determined by Lang et al (493 N)7 and Wang et al (522 N)17. The geometric conditions were comparable although the implant types were different, but in their complex simulations they used a higher torque (32 Ncm).This suggests that realistic preloads were used in the present investigation. Additionally, the interface between the implant and embedding material was modeled with fixed contact. Therefore, the detachment of the implant from the resin observed in load tests by Dittmer et al23 was not allowed, and the model must have exhibited slightly stiffer behavior than the experimental analog. Finally, since valid friction coefficients for lubricated titanium contact pairs are highly dependent on special surface conditions, a range of values was chosen, in accordance with data from the available literature. This might have resulted in stresses which are not absolutely valid for the individual situation but most probably reflects the consequences of lubricating the implant parts to be assembled.

Contrary to comparable investigations assuming linear elastic material behavior, the present study considered the possible plastic behavior of metal parts by introducing bilinear stress-strain curves for the respective materials. This enabled a realistic assessment of the extent of eventual plastic deformation after functional loading.

Even after screw tightening, considerable stresses arose in the vicinity of the contact faces. These were highly dependent on the friction coefficient and preload. While stresses were relatively moderate for the case of high friction (μ=0.5), they increased with a decreasing friction coefficient, approximately proportionally to the corresponding increases in preload. These results show that the tightening process cannot be neglected when stresses in dental implants are analyzed. During additional loading of up to 200 N at 30 degrees to the implant axis, the

tensional screw preload was gradually released until it reached about 60% of the starting value. The locations of maximum stress in the abutment shifted from the screw seat to the upper edge of the hexagon area opposite to the side of force application. Stress concentrations at this site were also found by Gehrke et al22 in an FEA of an implant with a zirconia abutment. Von Mises stresses in this area first decreased with a decreasing friction coefficient, reaching a minimum with μ=0.3, before increasing again; this is associated with a change in the character of stresses from tensile to compressive, as seen on closer examination of principal stresses. Since von Mises equivalent stresses are always positive, they do not distinguish between tensile (positive) and compressive (negative) stresses and may show a minimum value, as was the situation here, when principal stresses, from which they are calculated, exhibit a change in sign, corresponding to a change in character. Therefore, the maximum von Mises stress of 342 MPa at μ=0.5 in this area was associated with a maximum tensile stress of 451 MPa, and the maximum von Mises stress of about 320 MPa at μ=0.2 corresponded to a maximum compressive stress of approximately 302 MPa. This significant local shift in the nature of stresses demonstrates the major influence of friction and underlines the necessity of carefully considering frictional conditions in the FEA analyses of dental implants under load.

In the implant body, the most severe stresses after external loading developed at the implant neck in an area where the implant wall supports the abutment against the bending momentum exerted by the horizontal force component. In the present study, the von Mises stresses exceeded the materials' yield strength, indicating that plastic deformation is most likely to occur in this region. In in vitro load tests with the same implant type as used in the present study, once with titanium23 and once with zirconia abutments,32 plastic deformation at the implant neck was also observed after failure.23, 32

According to the load-displacement-curves recorded, plastic deformation was estimated to set in at a load of around 430 N (Dittmer et al23) or 500 N (Apicella et al32). These forces seem to be high compared to the 200 N which - according to the analyses presented - leads to stresses exceeding yield strength. However, the onset of plastic deformation cannot be precisely detected. Dittmer et al23 for example, defined the onset as the force at which the load-displacement curves deviated by more than 10% from the initial straight line, which is somewhat arbitrary and may easily have led to an overestimation of the respective force. However, because of simplifications and partly differing boundary conditions (Apicella et al32 applied a 45-degree load to a bare abutment without load cap), discrepancies between the model and experiment may have arisen. Nevertheless, in other implant systems too, the neck region seems to be at risk of plastic deformation at higher loads - as was observed experimentally by Coppede et al33 and in an FEA study by Gehrke et al.22 According to the results of the present study, this area of possible plastic deformation at the implant neck might expand considerably when saliva is present during implant assembly, thus reducing the interfacial friction between the implant components. Similar behavior may occur due to the repeated insertion and removal of the abutment screw, as described by Guzaitis et al.8 In this study, the friction coefficient decreased after multiple screw insertion cycles. This effect could also lead to higher stresses at the implant neck. Furthermore, studies examining the influence of repeated screw tightening and loosening or microgap formation should consider the influence of lubricants.

The finite element model presented here proved to be an effective tool for evaluating stresses in a loaded dental implant complex as a function of tribological conditions during implant assembly. It can easily be adapted to different problems in future investigations, for example, to study gap formation at the interface between the fixture and abutment or the effect of

changes in geometry or loading conditons. However, assessing the influence of frictional properties on stresses under cyclic loading under clinical conditions requires a completely different simulation design and further knowledge of material properties related to fatigue.

Conclusions

In this study, the numerical simulation of a dental implant showed that the friction coefficient has a major influence on screw preload and stresses in the implant system, both after preloading and after additional functional loading. However, after screw preloading, no plastic deformation could be observed in either implant or abutment for the range of friction coefficients considered. Additional oblique loading caused plastic deformation at the implant neck, in an area which expanded with a decreasing friction coefficient. Furthermore, reduced friction due to the the presence of saliva during the assembly of the implant and abutment is likely to have a detrimental effect on stresses in the implant components and should therefore be avoided. Therefore, in the instructions for use, screw tightening torques should be given for different surface conditions.

REFERENCES

1. McGlumphy EA, Mendel DA, Holloway JA. Implant screw mechanics. Dent Clin North Am 1998;42:71-89.

2. Hurson S. Practical clinical guidelines to prevent screw loosening. Int J Dent Symp 1995;3:22-5.

3. Patterson EA, Johns RB. Theoretical analysis of the fatigue life of fixture screws in osseointegrated dental implants. Int J Oral Maxillofac Implants 1992;7:26-33.

4. Haack J, Sakaguchi R, Sun T, Coffey J. Elongation and preload stress in dental implant abutment screws. Int J Oral Maxillofac Implants 1995;10:529-36.

5. Breeding LC, Dixon DL, Nelson EW, Tietge JD. Torque required to loosen single-tooth implant abutment screws before and after simulated function. Int J Prosthodont 1993;6:435-9.

6. Benac DJ. Technical brief: Avoiding bolt failures. J Fail Anal and Prev 2007;7:79-80.

7. Lang LA, Kang B, Wang R-F, Lang BR. Finite element analysis to determine implant preload. J Prosthet Dent 2003;90:539-46.

8. Guzaitis KL, Knoernschild KL, Viana M. Effect of repeated screw joint closing and opening cycles on implant prosthetic screw reverse torque and implant and screw thread morphology. J Prosthet Dent 2011;106:159-69.

9. Bickford JH. An introduction to the design and behavior of bolted joints: Marcel Dekker Inc. New York; 1995: 951p.

10. Buckley DH, Johnson, RL. Friction, wear, and adhesion characteristics of titanium-aluminium alloys in vacuum. Washington, D. C.: NASA; 1966: 16p.

11. Burguete RL, Johns RB, King T, Patterson EA. Tightening characteristics for screwed joints in osseointegrated dental implants. J Prosthet Dent 1994;71:592-9.

12. Tian H, Saka N, Suh NP. Boundary lubrication studies on undulated titanium surfaces. Tribol T 1989;32:289-96.

13. Seitzman LE, Bolster RN, Singer IL. IBAD MoS2 lubrication of titanium alloys. Surf Coat Tech 1996;78:10-3.

14. Abkowitz S, Burke, J.J., Hiltz, R.H. Titanium in industry. New York: Van Nostand Co Inc; 1955: 224p.

15. Budinski K. Tribological properties of titanium-alloys. Wear 1991;151:203-17.

16. Alkan I, Sertgöz A, Ekici B. Influence of occlusal forces on stress distribution in preloaded dental implant screws. J Prosthet Dent 2004;91:319-25.

17. Wang R-F, Kang B, Lang LA, Razzoog ME. The dynamic natures of implant loading. J Prosthet Dent 2009;101:359-71.

18. Saidin S, Abdul Kadir MR, Sulaiman E, Abu Kasim NH. Effects of different implant-abutment connections on micromotion and stress distribution: Prediction of microgap formation. J Dent 2012;40:467-74.

19. Wu T, Liao W, Dai N, Tang C. Design of a custom angled abutment for dental implants using computer-aided design and nonlinear finite element analysis. J Biomech 2010;43:1941-6.

20. Chun HJ, Shin HS, Han CH, Lee SH. Influence of implant abutment type on stress distribution in bone under various loading conditions using finite element analysis. Int J Oral Maxillofac Implants 2006;21:195-202.

21. Pessoa RS, Muraru L, Junior EM, Vaz LG, Sloten JV, Duyck J et al. Influence of implant connection type on the biomechanical environment of immediately placed implants - CT-based nonlinear, three-dimensional finite element analysis. Clin Implant Dent Relat Res 2010;12:219-34.

22. Gehrke P, Dhom G, Brunner J, Wolf D, Degidi M, Piattelli A. Zirconium implant abutments: fracture strength and influence of cyclic loading on retaining-screw loosening. Quintessence Int 2006;37:19-26.

23. Dittmer S, Dittmer MP, Kohorst P, Jendras M, Borchers L, Stiesch M. Effect of Implant-Abutment Connection Design on Load Bearing Capacity and Failure Mode of Implants. J Prosthodont 2011;20:510-6.

24. Guda T, Ross TA, Lang LA, Millwater HR. Probabilistic analysis of preload in the abutment screw of a dental implant complex. J Prosthet Dent 2008;100:183-93.

25. Merz B, Hunenbart S, Belser U. Mechanics of the implant-abutment connection: an 8-degree taper compared to a butt joint connection. Int J Oral Maxillofac Implants 2000;15:519-26.

26. International Organization for Standardization (editor). ISO 17862: 2012-03: Titanium and titanium alloy bars-Technical specifications. Geneva: International Organization for Standardization; 2012. http://www.beuth.de/de/norm/din-17862/148007096.

27. ASM International. Materials and coatings for medical devices: Cardiovascular. Ohio: ASM International; 2009.

28. International Organization for Standardization (editor). ISO 14801:2007: Dentistry - Implants - Dynamic fatigue test for endosseous dental implants. Geneva: International Organization for Standardization; 2007. http://www.iso.org/iso/catalogue_detail.htm?csnumber=41034.

29. Jörn D, Waddell J, Swain M. The influence of opaque application methods on the bond strength and final shade of PFM restorations. J Dent 2010;38 Suppl 2:e143-9.

30. Kanbara T, Yajima Y, Yoshinari M. Wear behavior of tetragonal zirconia polycrystal versus titanium and titanium alloy. Biomed Mater 2011;6:021001: 6pp.

31. Keith O, Kusy RP, Whitley JQ. Zirconia brackets: an evaluation of morphology and coefficients of friction. Am J Orthod Dentofacial Orthop 1994;106:605-14.

32. Apicella D, Veltri M, Balleri P, Apicella A, Ferrari M. Influence of abutment material on the fracture strength and failure modes of abutment-fixture assemblies when loaded in a bio-faithful simulation. Clin Oral Implants Res 2011;22:182-8.

33. Coppede AR, Bersani E, de Mattos Mda G, Rodrigues RC, Sartori IA, Ribeiro RF. Fracture resistance of the implant-abutment connection in implants with internal hex and internal conical connections under oblique compressive loading: an in vitro study. Int J Prosthodont 2009;22:283-6.

Corresponding author:

Dr Philipp Kohorst

Department of Prosthetic Dentistry and Biomedical Materials Science

Hannover Medical School

Carl-Neuberg-Str. 1

30625 Hannover

E-mail: kohorst.philipp@mh-hannover.de

Acknowledgements

The authors thank Dentsply Implants (Mölndal, Sweden) for kindly providing geometry data of the implant system and for their further support.

Table I. Material data used for FEA. The values without reference were provided by the manufacturer of the implant system. Tangent moduli were calculated from other properties given in the table.

Part	Material	Young Modulus [MPa]	Poisson Ratio	Yield Strength [MPa]	Ultimate Strength [MPa]	Ultimate Strain [%]	Tangent Modulus [MPa]
Abutment, Implant	Titanium, Grade 4	105 000	0.36	483	550	15 (26)	461
Abutment screw	Ti-6Al-4V	120 000	0.36	930	1,095	18 (27)	958
Embedding resin	PUR (Alpha Die)	3 525 (23)	0.33 (23)				
Load cap	CoCr alloy	190 500 (29)	0.26 (29)				

Table II. Number of tetrahedral elements for each part in model

Part	Number of Elements
Implant	60 796
Abutment	99 739
Abutment screw	73 319
Loading cap	91 209
Embedding resin	22 452

Table III. Screw preload as function of friction coefficient according to Equation 3

Friction Coefficient	Screw Preload [N]
0.2	506
0.3	353
0.4	271
0.5	219

Legends

Fig. 1. CAD model of implant body in embedding resin, abutment, abutment screw, and load cap in loading situation set up according to ISO 14801.28 The oblique load F is transferred to implant-abutment complex via hemispherical load cap with radius 4 mm and center at 11 mm above resin surface.

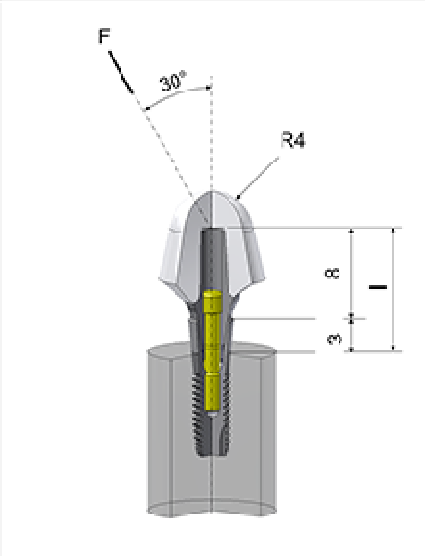

Fig. 2. Half-view of meshed model (load cap and embedding resin removed for clarity).

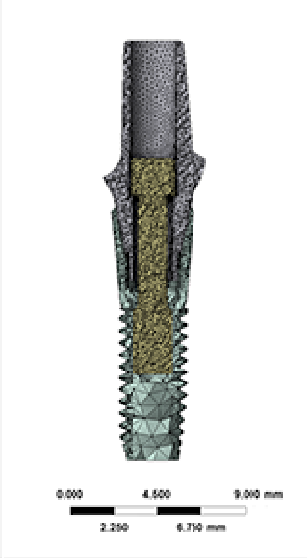

Fig. 3. Screw shaft force during first and second load steps

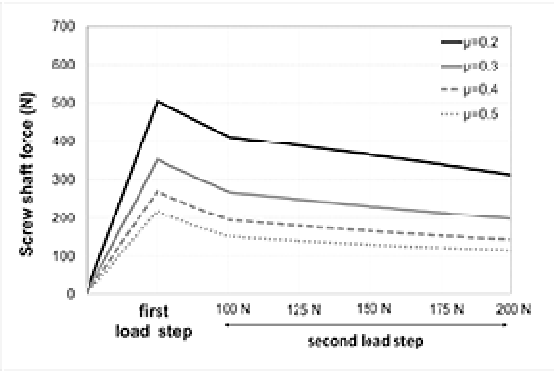

Fig. 4. Distributions of von Mises stresses on cross-sectional views of abutment after screw tightening (upper row) and oblique loading with 200 N (lower row) as function of friction coefficient.

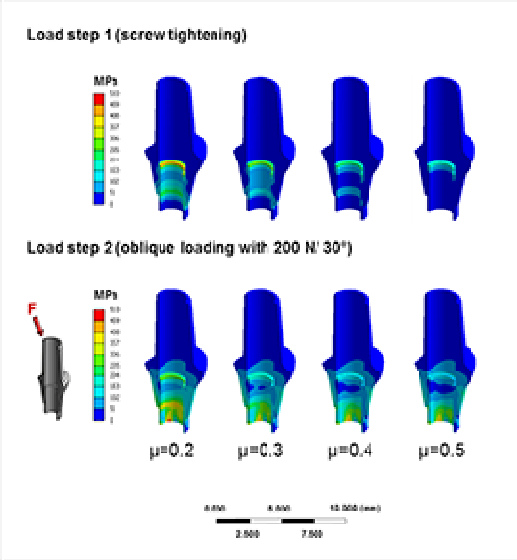

Fig. 5. Von Mises stresses after oblique loading with 200 N along upper edge of abutment hexagon as a function of friction coefficient; path of evaluation is marked with black arrow on left.

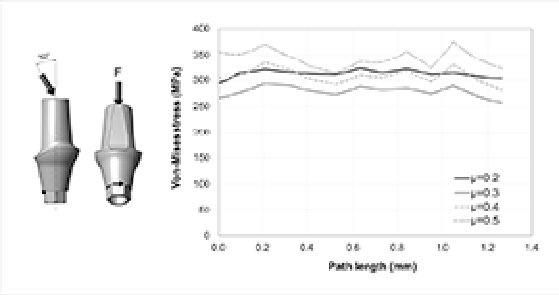

Fig. 6. Distributions of von Mises stresses on cross-sectional views of implant after screw tightening (upper row) and oblique loading with 200 N (lower row) as function of friction coefficient.

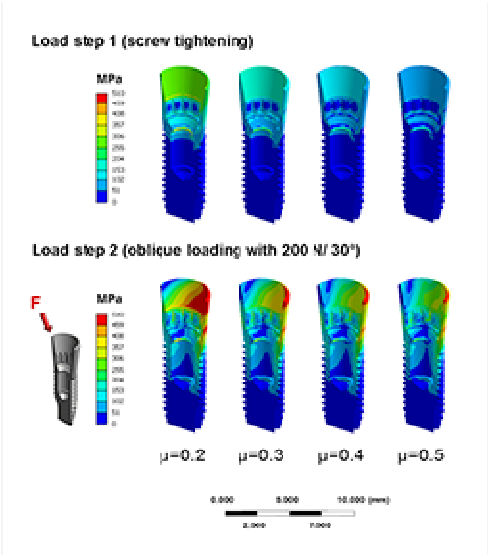

Fig. 7. Von Mises stress at upper edge of conical implant opening after screw tightening as function of friction coefficient; path of evaluation is marked with dotted line on left.

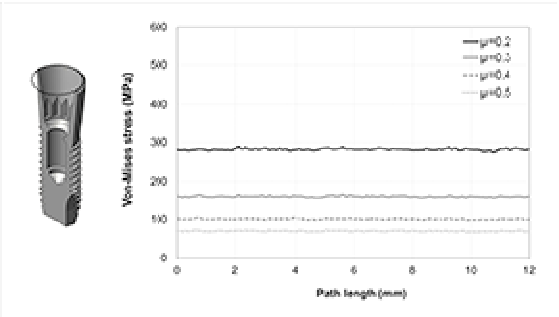

Fig. 8. Von Mises stress at upper edge of conical implant opening after oblique loading with 200 N; path of evaluation is marked with dotted line on left.